Optical Properties of ChR2

Stephen Allen

Major Qualifying Project

Advisor: Dr. Robert E. Dempski

Table of Contents

Abstract

Channelrhodopsin-2 (ChR2) is a light activated cation channel permeable to monovalent and divalent ions [1,2,3]. It was first discovered in the green algae *Chlamydomonas reinhardtii* where it is implicated in phototactic response [4,3]. ChR2 is a microbial-type rhodopsin with seven transmembrane (TM) domains and the chromophore all-trans-retinal bound to a single lysine residue on TM7 [5]. Channel activation occurs upon photoisomerization of retinal to 13-cis with blue light [1]. The maximal response of wild-type ChR2 occurs with 470 nm light (λ_{max}) [1,4]. ChR2 has been used to create action potentials and signaling events from a light pulse, a newly developing field labeled "optogenetics" [6,7]. ChR2 can be used as a tool to map neuronal networks and in the future has been proposed to be used to cure blindness [8]. Wild type ChR2, however, does not have favorable properties to fully utilize this protein [6,7]. One area of interest is to make ChR2 more plausible for use is the shifting of its λ_{max} [9]. The electrostatic environment near the retinal binding has been shown to influence the maximal absorbance of retinal in both ChR2 and the well understood bacteriorhodopsin [10].

We hypothesized that charged amino acids mutations centered at G181, which sits proximal to the β-ionone ring of retinal, would alter the electrostatic environment of the retinal binding pocket and therefore influence the λ_{max} of ChR2 [1,10] (Figure 1). Glycine was mutated to serine, threonine, lysine, aspartic acid and glutamic acid. Action spectrum were recorded by measuring maximal current responses with two-electrode voltage clamp as a function of wavelength using tunable bandpass filters [11]. We found that G181S and G181T had little to no effect on λ_{max} but showed reduced function. Additionally, all charged mutants had little or no activation, which was shown to be a consequence of surface expression by Western blotting. Therefore, we suggest that G181 is important for the proper surface expression of ChR2.

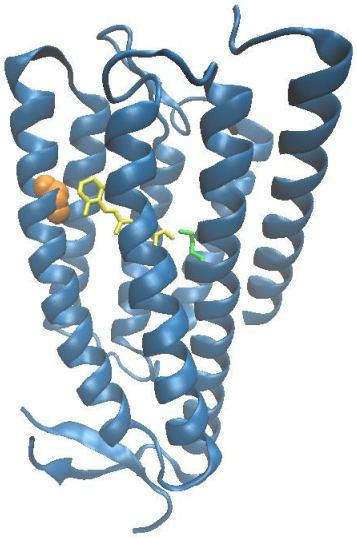

Figure 1 - Crystal Structure of channelrhodopsin chimera C1C2 (PDB entry: 3UG9) highlighting the site of Quikchange mutagenesis. Residue G181 is shown in orange. Retinal chromophore shown in yellow bound to K257 denoted by green color . The figure was created using Visual Molecular Design [12]

.

Introduction

Ion channels, transporters, and pumps are critical membrane proteins that facilitate the exchange and movement of molecules across cellular membranes [13,14,15]. Channels are responsible for expeditious, large changes in ionic composition while transporters and pumps act in a slower fashion. Although pumps and channels have widely differing mechanisms of ion transport, the structural differences may not be apparent.

The polarization of the cell caused by the change in ionic concentrations facilitated by ion pumps, channels and carriers has been shown to play a vital role in intracellular signaling, cell volume regulation and numerous additional biological processes [16]. Most channels contain a gating mechanism that determines whether the channel is in an open or closed state [14]. Ion channels are often classified by what stimulation transitions the channel between the open and closed state [15]. Channels function by allowing passive diffusion of ions down the electrochemical

gradient through an open pore upon activation [14,15]. The amino acid composition in addition to the size of the pore determines the selectivity for specific ions to permeate at speeds very close to that of the rate of diffusion for the molecule [14,17]. In contrast to channels, ion pumps transport molecules against the electrochemical gradient in an energetically unfavorable process which requires energy input [16]. The transport mechanism for ion pumps is drastically different from channels. Instead of a continuous pore, ions are transported via binding, occlusion and release [16]. Therefore, pumps move ions at a rate orders of magnitude slower compared to channels.

Interestingly, although the mechanisms for ion transport are largely different between ion channels and pumps, the secondary structures can be very similar. This is evident in the ClC family of channels and pumps. The general crystal structure of the ClC apoprotein is a dimer composed of 18 alpha helices tilted to the plane of the membrane (Figure 2) [18,19]. The ions are transported through a barrel structure located in each subunit of the dimer in both the channel and pump iosforms [20,21]. The two classes, channels and pumps, are separated by the slight timing difference in the open to closed state of the intracellular and extracellular gates [16].

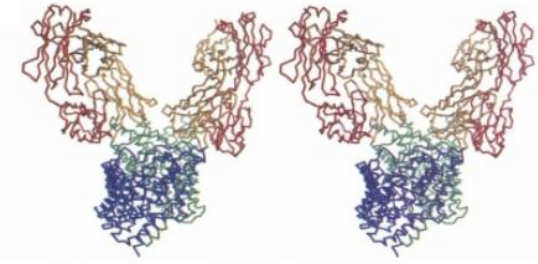

Figure 2 - Crystal Structure of ClC dimer (PDB entries: 1KPK 1KPL). Each subunit forms a separate Cl pore to conduct the ions. Each subunit of the dimer is formed from 9 alpha helices tilted with respect to the plane of the membrane [21].

.

Extensive work on the light-activated protein bacteriorhodopsin (bR) has provided valuable information on the structure of membrane proteins [22]. Bacteriorhodopsin is a microbial-type rhodopsin comprised of seven transmembrane helices and the cofactor all-trans-retinal bound to a conserved lysine residue through a Schiff base covalent bond [23]. The light sensing

retinal moiety is responsible for the activation of the pump where maximal activation occurs at 570 nm [22]. Upon the absorption of a photon of 570 nm light, retinal photoisomerizes to 13-cis, allowing for proton efflux to occur [24],[23]. Conformational changes occur in bR once the Schiff base has protonated Asp-85 [25]. As the retinal isomerizes, the Schiff base proton is transferred to the Asp-85 residue in the bacteriorhodopsin on the extracellular side. Following this step, a proton is released to the intracellular side of the cell [22]. The photocycle is completed by the re-protonation of the Asp-96 residue and the re-isomerization of the retinal to all-trans [22,26]. The movement of protons allows the cell to build up a gradient across the membrane of the cell allowing for ATP synthesis within the cell [26].

In recent years a new microbial-type rhodopsin, channelrhodopsin-2 (ChR2), was molecular defined in the green algae *Chlamydomonas reinhardtii* [4,3]. Together with channelrhodopsin-1 (ChR1), ChR2 functions to facilitate phototaxis in the algae. Similar to bR, ChR2 is comprised of seven transmembrane domains with the retinal chromophore covalently bound to a lysine at position 257 (Figure 1) [2,10]. However, unlike bR, ChR2 functions mainly as a mono- and divalent cation channel and not a pump [2]. However, there is evidence that ChR2 can also act as a proton pump in the absence of an electrochemical gradient [2]. Therefore, it has been suggested that ChR2 is a proton pump with an inherent leak current that mimics ion channel properties [2]. In comparison to bR, ChR2 activation is blue shifted with a λ_{max} of 470 nm [8].

A major residue integral for the first step in the photocycle of ChR2 is K257 which links the retinal moiety to the protein [1]. After protonation of the Schiff base by E123 the proton is passed to D253 [1]. The photocycle is then completed by the transfer of a proton back to the Schiff base by D156 [27]. Mutation of D253 to alanine had a delayed activation and produced almost zero photocurrent despite large membrane expression [1]. E123 has also been shown to be important

for proper channel function. Mutations of this amino acid to Thr or Ala cause the channel to close at an accelerated rate compared to the wild type [1].

Another consequence of a mutation to a residue close to the retinal is a shift in the λ_{max} of ChR2 [1]. This is due to the mutation altering the counter ion near the Schiff base, the increase of the electric field surrounding the Schiff base, the induction of twisting of the chromophore, alterations to the hydrogen bonding networks [27]. Already there have been mutations to key residues that have altered this value. Another approach to alter the λ_{max} has been to use varying pieces of channelrhodopsin helices to produce the desired properties [17]. These mutants could potentially be used as a tool for neuronal mapping and activation [28]. A goal of ChR2 mutants is to create ChR2 variants that can be activated and turned off to polarize and depolarize the cell membrane at various wavelengths [28,29,4]. The current λ_{max} of ChR2 in the blue region of light scatters the light in biological tissue requiring a high intensity of light to activate the channel [4]. One example of this occurring is a mutation of E123. It was proved that by mutating this residue to a Thr or Ala the λ_{max} of ChR2 would a red shift the λ_{max} by 20nm [1].Another residue near the binding pocket is H134. When this residue was mutated to Arg a blue shift was observed in the λ_{max} by 20 nm [30].

A channelrhodopsin chimera formed from helices originating from the various organisms from which this class of protein has been isolated from has shown shifts to the λ_{max}. A chimera of the channelrhodopsin-1 (ChR1) and ChR2 protein has produced a red shifted λ_{max} from the wild type at 500 nm [31]. Another chimera that has produced a red-shifted protein was produced from the fusion of a ChR1 and *Volvox carteri* ChR1. This produced a shift in the λ_{max} centering the maxima at 560 nm [32].

Recently, mutation of G181 to serine was shown to have decreased conductance, reduced permeability and pore diameter [33]. G181 is located proximal to the β-ionone ring of retinal [33,1]. It has been shown that photoactive proteins hold potential use in the field of optogenetics [8,9,32]. This field involves transfecting organisms with photoactive proteins allowing for selective activation and deactivation through a light pulse of a certain wavelength. Upon activation a membrane potential builds in the cell allowing for the selective firing of neurons leading to the possibility for mapping. We hypothesized that by introducing charged residues at this location they would alter the electrostatic environment around retinal therefore shifting the maximal absorbance of ChR2. A more extensive study of this residue was carried out through the introduction of a Lys, Asp, Glu, and Thr at position 181. These mutants were then expressed in *Xenopus laevis* oocytes [11,34]. The oocytes, after recovery, were then analyzed using two electrode voltage clamp method to obtain current vs time traces for wavelengths of various values using bandpass filters [33]. Three of the mutants analyzed proved to be nonfunctional. One, however, the G181T, was functional. A potential shift for λ_{max} was then examined through action spectrum analysis although none was determined. The non-functional mutants were further tested for surface expression using Western blotting techniques [33]. It was found that G181 is a critical residue for proper surface expression of ChR2. These results demonstrated that the mutations chosen at G181 did not produce a spectral shift in the λ_{max}.

Materials and Methods

Animal Subjects Involved

Oocytes from the *Xenopus laevis* were isolated according the guidelines given in the Guide for the Care and Use of Laboratory Animals of the National Institutes of Health [34]. The surgical

procedure that was used was approved by the WPI Institutional Animal Care and Use Committee.

Reagents

Restriction enzymes were purchased from New England Biolabs, Inc. (Ipswich, MA). From Macherey-Nagel (Bethlehem, Pa) the Nucleic Acid and Protein Purification kit were obtained. A Quikchange site-directed mutagenesis kit was bought from Stratagene. (La Jolla, CA). A High Pure PCR Product Purification Kit was bought from Roche (Indianapolis, IN). Any other reagents listed were purchased from Sigma-Aldrich Corp. (St. Louis, MO) unless differently stated.

Molecular Biology

A truncated wild type channelrhodopsin-2 (ChR2, amino acids 1-309) with the hemagluttanin (HA) epitope sequence (YPYDVPDYA) was unidirectionally cloned into the vector pTLN using the *Xba1*and *EcoRV* restriction sites. Threonine, Glutamic Acid, Aspartic Acid and Lysine mutations were introduced at residue number 181 using the Quikchange site-directed mutagenesis. The mutations were verified using full gene sequencing from Macrogen.

Oocyte Preparation and mRNA Synthesis

Oocytes were isolated according to pre-established methods [34]. In brief, oocytes were digested with collagenase (3 mg/mL for three hours at 17º Celsius) in ORI^{+} solution (90 nM NaCl, 2 mM KCl, 2 mM $CaCl_2$, 5 mM MOPS; pH 7.4) after partial overactomy of the *Xenopus laevis*. ChR2 mRNA was generated with the SP6 mMessage and mMachine kit according to the manufacturer's instructions. A volume of 50 nL of 1 ug/ul mRNA was injected into each oocyte

and incubated in ORI^{+} solution with 1 mg/mL gentamycin and 1 uL all-trans retinal (1 mM stock in DMSO) in the dark for three days at 17º.

Oocyte Membrane Preparation and Western Blotting

Xenopus oocyte total membrane fractions were prepared as described previously [11,35]. Briefly, oocytes were homogenized in 20 µL/oocyte homogenization buffer A (20 mM Tris, 5 mM $MgCl_2$, 5 mM NaH_2PO_4, 1 mM EDTA, and 80 mM sucrose; pH 7.4) supplemented with 1 mM PMSF, Homogenized oocytes were spun at 200 g for 5 minutes at 4°C. The supernatant was drawn off and placed into a separate 1.5 mL eppendorf tube then spun at 14,000 g for 20 minutes at 4°C to pellet the membrane. The membrane pellet containing the protein was solubilized in 4 µl/oocyte Laemmli buffer and incubated at 37°C for 45 minutes for denaturing [33]. Protein samples were separated on a 12% gel using SDS-PAGE and transferred onto PVDF membranes. The membranes were blocked in 5% nonfat milk overnight at 4°C. Blocked membrane were incubated with anti-HA polyclonal antibody (1:1000; Thermo Fisher Scientific, Waltham, MA) for 45 minutes at room temperature. Membranes were washed 3 times for 5 minutes in solution containing TBST (0.5% tween) and following that incubated with an AP conjugated anti-rabbit secondary antibody (1:5000; Rockland Inc., Gilbertsville, PA) for 45 minutes at room temperature. The membrane was then washed again once solution containing TBST (0.5% tween) and twice with TBS for five minutes each. The ChR2 band was visualized using developing solution (Bio-Rad Laboratories Inc., Waltham, MA) [33,34].

Electrophysiology

A PC-10 pipette puller (Narishige, Japan) was used to pull microelectrodes from borosilicate glass capillaries (World Precision Instruments, Sarasota, Florida). The resistance on

the microelectrodes ranged from 0.5 to 2 MΩ. After the incubation at 17º C for three days in the dark oocytes were placed in an RC-10 oocyte chamber (Warner Instruments, LLC; Hamden, Connecticut). A 115 mM NaCl, 2 mM $BaCl_2$, 1 mM $MgCl_2$, 5 mM tris base solution at pH 9.0 was introduced to the chamber through a VC-6 6 channel perfusion valve control system (Warner Instruments LLC; Hamden, Connecticut). ChR2 was activated with a 75 W xenon arc lamp (Specialty Optical Systems, Inc., Dallas, Texas) and a 2 mm light guide (~4×10^{21} photons s^{-1} m^2). The currents were measured using a Turbo-Tec 03X amplifier (npi electronic GmbH, Germany) set to voltage clamp mode. The membrane potential was set to -40 mV. The oocytes were exposed to lights of wavelengths from 440 nm to 560 nm using bandpass filters from Edmund Optics. The oocytes were also subjected to light that passed through various optical density filters (Thor labs). Data was recorded using pClamp10 software (Axon Instruments, Inc., Burlingame, California) and further analyzed using Clampfit 10.2 and SigmaPlot. Light-induced currents were normalized to the highest recorded response and monitored for a shift in lambda max from the wild type. This was done through a comparison of wild type cells measured on the same day to the mutant in question graphed in Microsoft Excel using value obtained from the Clampfit 10.2 software.

Results

To examine shifts to the lambda max of ChR2, four mutations were introduced at a site near the retinal binding pocket at position 181., Previous research has shown this residue has an effect on channel function, but it was unknown if a chromatic shift could be induced at this residue [33]. G181 was mutated to G181S, G181T, G181E, G181D, and G181K to alter the electrostatic environment surrounding the retinal. These mutant constructs were subsequently

expressed in *Xenopus laevis* oocytes. Two-electrode voltage clamp was used to record photocurrent response at various wavelengths of light ranging from 430 nm – 550 nm.

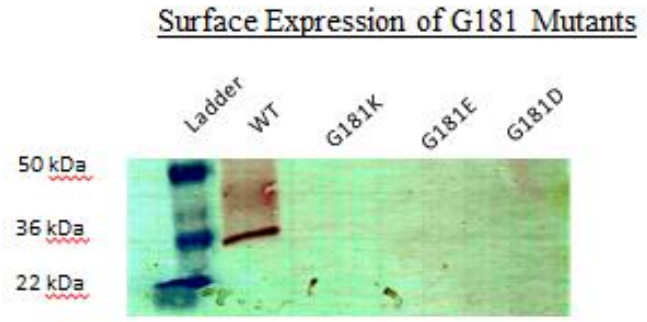

Figure 3 - Western Blot of G181K, G181E, and G181D mutants ran against WT. ChR2-HA tagged band appears at ~35 kDa. The WT was the only lane to show a band indicating reduced surface expression in the mutants of ChR2.

The G181E, G181K and G181D mutants proved to be nonfunctional as shown by the current traces (Figure 4). Compared to WT ChR2 on the same day, no current response is detected after excitation with light. To determine whether the lack of function was caused by surface expression or a non-functional ChR2, Western blotting was performed (Figure 3). We observed that WT ChR2 had expression as expected at ~35 kDa. Each of the mutants, however, failed to produce a band at this location. This suggests that these mutants have no surface expression in oocytes.

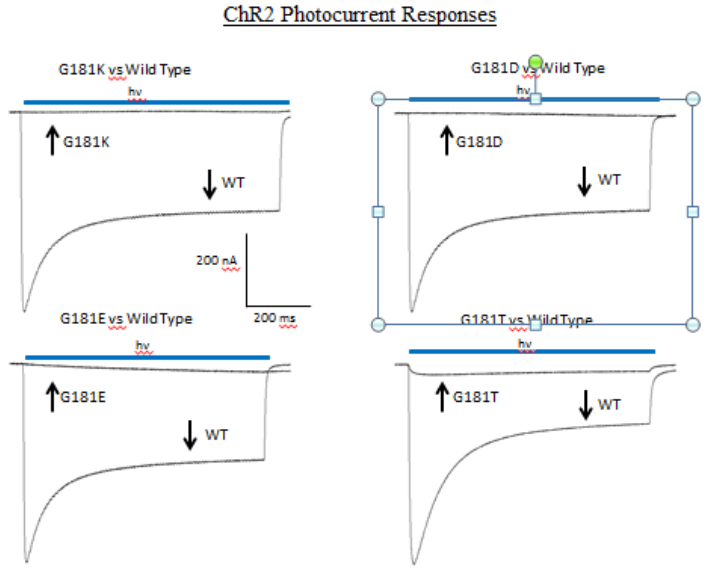

Figure 4 - Photocurrent Response of G181K, G181E, G181D, and G181T compared to WT on the same day. The G181K, G181E, G181D mutants all proved to be nonfunctional as shown by the lack of photoinduced current. The G181K mutant proved to be a functional mutant as shown by the photoinduced current. The function was diminished as can be seen by the comparatively small response of the mutant to WT.

G181T produced a functional mutant with currents that resembled the phenotype. However, the current responses were less than those of WT ChR2 by approximately 70% (Figure 5).

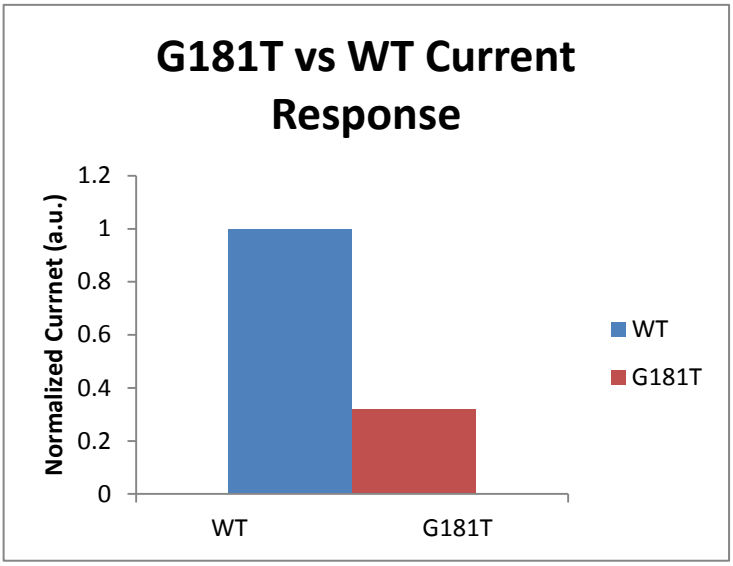

Figure 5 - Normalized current response for WT and G181T. Photocurrent responses were averaged and normalized to WT on the same day. The G181T proved to show 70% reduced function to WT.

We recorded photocurrents as a function of wavelength using tunable bandpass filters. From maximal current responses, action spectra were created to determine the wavelength maximum (Figure 6). The data was fitted to a normal Gaussian distribution to determine the λ_{max}. The λ_{max} of WT ChR2 was 482 nm and the λ_{max} of G181T was 492 nm.

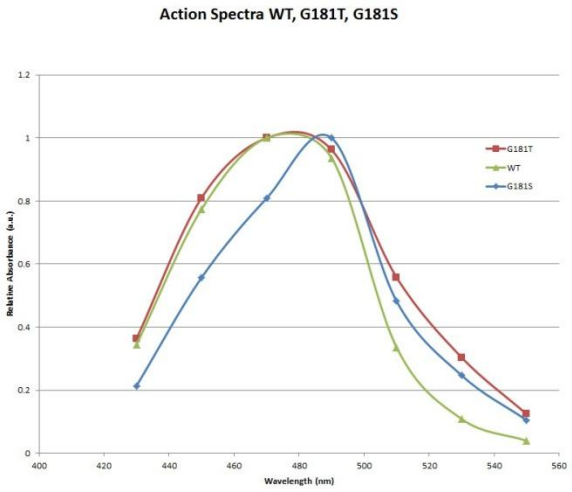

Figure 6 - Action spectra of functional G181 mutants. Spectra were recorded as described in Materials and Methods. Each data point is the averaged normalized response for a given wavelength (± SEM; n>=3). Mutants proved to show no shift to λ_{max} when compared to WT.

Another functional mutant was produced by the G181S mutation. Like G181T, the current response was reduced [33]. The action spectrum also revealed no change to the λ_{max} of

ChR2 [33].

Discussion

The optical properties of ChR2 allow for the protein to have many potential uses in the field of optogenetics [29]. Mutants have been produced that shift the spectral properties of the ChR2 which can be attributed to multiple advances in the field of optogenetics [29]. Mutations to residues in close proximity to the retinal have been shown alter the λ_{max} of the protein [8]. This could potentially lead to researches creating mutations that activate the ChR2 protein at various wavelengths allowing for neuronal activation and the mapping of pathways. This is a direct result of ChR2 being a photoactive protein. When the ChR2 detects a light pulse of a specific wavelength and activates, an ion gradient builds within the cell which could be used to create an action potential[7,8,30].

The main hypothesis of this project was that an optical shift could be established in ChR2 through introduction of charged or polar mutants at G181. No experimentally significant shifts were observed although other properties of this residue can be inferred from the results.

The first of these conclusions is that the G181 residue is important for proper trafficking of the ChR2 protein to the plasma membrane of the cell. This claim is supported by all mutants produced. Three of the mutants proved to be nonfunctional (G181K, G181E, G181D) as shown through the lack of an induced current upon a light pulse. This lack of a response was further explained using a western blot to test for surface expression. Upon visualization of the developed gel using both a primary anti-HA antibodies and a secondary anti-rabbit antibody there appears no band corresponding to that produced by the WT ChR2. This result shows that these mutant

ChR2 constructs are not present on the surface of the cell membrane which supports the claim that G181 is an important residue for proper surface expression of ChR2.

This claim that G181 is an important residue for proper trafficking of ChR2 to the surface of the plasma membrane was also supported by the functional mutants G181S and G181T. As shown in Figure 1 the mutant produced a greatly reduced response to the light pulse in comparison to that shown by the wild type. Although no Western blotting for surface expression was performed, we speculate that these mutants will have expression proportional to function.

Another conclusion that can be drawn from the results is that no alteration to the λ_{max} of ChR2 occurs with the given mutations. As previously stated the G181K, G181E, G181D mutants were nonfunctional leading to no activation of the protein nullifying any potential shift in λ_{max}. The G181T mutant data also supported this conclusion. The action spectrum revealed in Figure 5 exhibits a comparative λ_{max} to the wild type. The experimental λ_{max} value of 482 +- 2.5 nm is comparable to the theoretical value of 470 nm for WT ChR2 showing no change to λ_{max}.

It is possible that the size and polarity of our mutations cause the lack of function for ChR2. Non-polar and smaller residues could be introduced in an attempt to create a shift in λ_{max} with proper function. Possible mutants include Val, Met, Ala and Leu.

In conclusion, although no spectral shifts occurred with the mutations at G181 an important conclusion could be drawn about this residue; it is required for proper trafficking of ChR2 to the plasma membrane of the cell.

Bibliography

1. Kato HE, Hayashi S, Hegemann P, et al. Crystal structure of the channelrhodopsin light-gated cation channel. *Nature*. 2012;482(7385):369-U115. doi: 10.1038/nature10870.

2. Katrin Feldbauer, Dirk Zimmermann, Verena Pintschovius, Julia Spitz, Christian Bamann, Ernst Bamberg. Channelrhodopsin-2 is a leaky proton pump. *Proc Natl Acad Sci U S A*. 2009;106(30):12317-12322. doi: 10.1073/pnas.0905852106.

3. Radu I, Bamann C, Nack M, Nagel G, Bamberg E, Heberle J. Conformational changes of channelrhodopsin-2. *J Am Chem Soc*. 2009;131(21):7313-7319. doi: 10.1021/ja8084274.

4. Hou S, Govorunova EG, Ntefidou M, et al. Diversity of chlamydomonas channelrhodopsins. *Photochem Photobiol*. 2012;88(1):119-128. doi: 10.1111/j.1751-1097.2011.01027.x.

5. Watanabe HC, Welke K, Schneider F, et al. Structural model of channelrhodopsin. *The Journal of biological chemistry*. 2012;287(10):7456-7466. doi: 10.1074/jbc.M111.320309.

6. LIGHT-ACTIVATED CATION CHANNEL AND USES THEREOF. . 2006.

7. Kleinlogel S, Feldbauer K, Dempski R, et al. Ultra light-sensitive and fast neuronal activation with the Ca2+-permeable channelrhodopsin CatCh. *NATURE NEUROSCIENCE*. 2011;14(4):513-U152. doi: 10.1038/nn.2776.

8. Prigge M, Schneider F, Tsunoda SP, et al. Color-tuned channelrhodopsins for multiwavelength optogenetics. *The Journal of biological chemistry*. 2012;287(38):31804-31812. doi: 10.1074/jbc.M112.391185.

9. Welke K, Frähmcke JS, Watanabe HC, Hegemann P, Elstner M. Color tuning in binding pocket models of the chlamydomonas-type channelrhodopsins. *The journal of physical chemistry.B*. 2011;115(50):15119-15128. doi: 10.1021/jp2085457.

10. Lórenz-Fonfría VA, Heberle J, Resler T, et al. Transient protonation changes in channelrhodopsin-2 and their relevance to channel gating. *Proc Natl Acad Sci U S A*. 2013;110(14):E1273. doi: 10.1073/pnas.1219502110.

11. Dürr KL, Tavraz NN, Zimmermann D, Bamberg E, Friedrich T. Characterization of na,K-ATPase and H,K-ATPase enzymes with glycosylation-deficient beta-subunit variants by voltage-clamp fluorometry in xenopus oocytes. *Biochemistry*. 2008;47(14):4288.

12. Humphrey W, Dalke A, Schulten K. VMD: Visual molecular dynamics. *JOURNAL OF MOLECULAR GRAPHICS & MODELLING*. 1996;14(1):33-38.

13. Abramson J, Smirnova I, Kasho V, Verner G, Kaback HR, Iwata S. Structure and mechanism of the lactose permease of escherichia coli. *Science (New York, N.Y.)*. 2003;301(5633):610-615.

14. Fermini B, Priest BT, SpringerLink ebooks - Chemistry and Materials Science. *Ion channels*. Vol 3. Berlin: Springer Berlin Heidelberg; 2008. 10.1007/978-3-540-79729-6.

15. Faller LD. Mechanistic studies of sodium pump. *Arch Biochem Biophys*. 2008;476(1):12-21. doi: 10.1016/j.abb.2008.05.017.

16. Gadsby DC. Ion channels versus ion pumps: The principal difference, in principle. *Nature Reviews Molecular Cell Biology*. 2009;10(5):344-352. doi: 10.1038/nrm2668.

17. Wang J, Ma M, Locovei S, Keane RW, Dahl G. Modulation of membrane channel currents by gap junction protein mimetic peptides: Size matters. *American journal of physiology.Cell physiology*. 2007;293(3):C1112-1119. doi: 10.1152/ajpcell.00097.2007.

18. Raimund Dutzler, Ernest B Campbell, Martine Cadene, Brian T Chait, Roderick MacKinnon. X-ray structure of a CIC chloride channel at 3.0 angstrom reveals the molecular basis of anion selectivity. *Nature*. 2002;415(6869):287. doi: 10.1038/415287a.

19. Accardi A, Picollo A. CLC channels and transporters: Proteins with borderline personalities. *BBA - Biomembranes*. 2010;1798(8):1457-1464. doi: 10.1016/j.bbamem.2010.02.022.

20. Jentsch TJ, Friedrich T, Schriever A, Yamada H. The CLC chloride channel family. *Pflügers Archiv : European journal of physiology*. 1999;437(6):783.

21. Dutzler R, Campbell EB, MacKinnon R. Gating the selectivity filter in ClC chloride channels. *Science (New York, N.Y.)*. 2003;300(5616):108-112. doi: 10.1126/science.1082708.

22. Lanyi JK. Bacteriorhodopsin. *Annu Rev Physiol*. 2004;66(1):665-688. doi: 10.1146/annurev.physiol.66.032102.150049.

23. Lozier RH, Bogomolni RA, Stoeckenius W. Bacteriorhodopsin: A light-driven proton pump in halobacterium halobium. *Biophys J*. 1975;15(9):955-962. doi: 10.1016/S0006-3495(75)85875-9.

24. Hofrichter J, Henry ER, Lozier RH. Photocycles of bacteriorhodopsin in light- and dark-adapted purple membrane studied by time-resolved absorption spectroscopy. *Biophys J*. 1989;56(4):693-706. doi: 10.1016/S0006-3495(89)82716-X.

25. Caspar DL. Protein microscopy. bacteriorhodopsin--at last. *Nature*. 1990;345(6277):666-667.

26. del Rosario RCH, Oppawsky C, Tittor J, Oesterhelt D. Modeling the membrane potential generation of bacteriorhodopsin. *Math Biosci*. 2010;225(1):68-80. doi: 10.1016/j.mbs.2010.02.002.

27. Lasogga L, Rettig W, Otto H, Wallat I, Bricks J. Model systems for the investigation of the opsin shift in bacteriorhodopsin. *The journal of physical chemistry. A*. 2010;114(5):2179-2188. doi: 10.1021/jp904132f.

28. Mancuso JJ, Kim J, Lee S, Tsuda S, Chow NBH, Augustine GJ. Optogenetic probing of functional brain circuitry. *Experimental Physiology*. 2010;96(1):26-33. doi: 10.1113/expphysiol.2010.055731.

29. Rein ML, Deussing JM. The optogenetic. *Molecular Genetics and Genomics*. 2012;287(2):95.

30. Lin JY, Lin MZ, Steinbach P, Tsien RY. Characterization of engineered channelrhodopsin variants with improved properties and kinetics. *Biophys J*. 2009;96(5):1803-1814. doi: 10.1016/j.bpj.2008.11.034.

31. Wang H, Sugiyama Y, Hikima T, et al. Molecular determinants differentiating photocurrent properties of two channelrhodopsins from chlamydomonas. *The Journal of biological chemistry*. 2009;284(9):5685-5696. doi: 10.1074/jbc.M807632200.

32. Yizhar O, Paz JT, Stehfest K, et al. Neocortical excitation/inhibition balance in information processing and social dysfunction. *Nature*. 2011;477(7363):171. doi: 10.1038/nature10360.

33. Richards R, Dempski RE. Re-introduction of transmembrane serine residues reduce the minimum pore diameter of channelrhodopsin-2. *PloS one*. 2012;7(11):e50018.

34. Richards R, Dempski RE. Examining the conformational dynamics of membrane proteins in situ with site-directed fluorescence labeling. *Journal of visualized experiments : JoVE*. 2011(51). doi: 10.3791/2627.

35. Kamsteeg EJ, Deen PM. Detection of aquaporin-2 in the plasma membranes of oocytes: A novel isolation method with improved yield and purity. *Biochem Biophys Res Commun*. 2001;282(3):683-683. doi: 10.1006/bbrc.2001.4629.